



# How does chlorine substitution on acetonitrile affect the internal $S_N2$ isomerization of proton-bound pairs $(\text{ClCH}_2\text{CN})(\text{ROH})\text{H}^+$ ( $\text{R} = \text{CH}_3, \text{C}_2\text{H}_5, \text{C}_3\text{H}_7$ )?

Richard A. Ochran, Paul M. Mayer\*

Chemistry Department, University of Ottawa, Ottawa, Canada K1N 6N5

Received 1 April 2002; accepted 31 July 2002

## Abstract

The unimolecular reactions of proton-bound pairs of chloroacetonitrile and a variety of alcohols (methanol, ethanol, *n*- and *i*-propanol) were studied in order to probe the impact of chloro-substitution on both the internal  $S_N2$  rearrangement leading to dehydration and simple hydrogen-bond cleavage reactions. Chloro-substitution on acetonitrile does not significantly affect the height of the highest energy isomerization barrier which governs the dehydration reaction but does reduce the relative energy of the transition state that leads to the formation of the high energy intermediate ion  $(\text{CH}_3\text{CH}\cdots\text{R}\cdots\text{OH}_2)^+$ . Kinetic modeling of the unimolecular reactions with RRKM theory showed that this latter reaction is a key step in governing the ratio of the two types of reactions observed in the MI mass spectra even though it is not the rate-limiting step for the overall isomerization mechanism leading to dehydration. Chloro-substitution also reduces the proton affinity of acetonitrile resulting in the lowest energy simple-bond cleavage reaction products to be  $\text{ROH}_2^+ + \text{ClCH}_2\text{CN}$  in all cases.

© 2003 Elsevier Science B.V. All rights reserved.

**Keywords:** Cluster ions; Unimolecular reactions; Chloro-substitution effects; Tandem mass spectrometry

## 1. Introduction

In three recent publications [1–3] mass spectrometry and ab initio calculations were employed to investigate the unimolecular decomposition of proton-bound pairs consisting of acetonitrile and the alcohols methanol, ethanol, *n*-propanol, *iso*-propanol, *n*-butanol, *s*-butanol, *iso*-butanol and *t*-butanol. Common to the chemistry of these pairs (on the microsecond time-scale) was the competition between simple hydrogen-bond cleavage and dehydration reactions. The

latter reaction channel involves an  $S_N2$ -type rearrangement with the initial isomerization of  $(\text{CH}_3\text{CN})(\text{ROH})\text{H}^+$  [ $\text{R} = \text{alkyl}$ ] to an intermediate  $(\text{CH}_3\text{CH}\cdots\text{R}\cdots\text{OH}_2)^+$  ion (via TSa) followed by the stretching of the C–O bond in this ion to form a thermodynamically stable isomer  $(\text{CH}_3\text{CNR})(\text{H}_2\text{O})^+$  (via TSb) (Scheme 1) [2–4].

The competition between dissociation and isomerization is a result of the similar barrier energies for the two processes. One question which arises is how universal such a competition will be when the monomeric units in the pair are modified by functional groups. If a moiety is used that affects the energetics of the simple-dissociation products, what

\* Corresponding author. Tel.: +1-613-562-5800;

fax: +1-613-562-5170.

E-mail address: [pmayer@science.uottawa.ca](mailto:pmayer@science.uottawa.ca) (P.M. Mayer).



Scheme 1.

will be the effect on the transition state leading to the  $\text{S}_{\text{N}}2$  isomerization products? The previous work examined the methyl-substitution effects on the central carbon in the  $(\text{CH}_3\text{CH}\cdots\text{R}\cdots\text{OH}_2)^+$  ion. Sequential methyl substitution stabilized this ion and TSa, but only dimethyl-substitution lowered the relative energy of the rate-limiting TSb [3]. To further examine this aspect of the competition in nitrile–alcohol clusters, we have studied the unimolecular decomposition of proton-bound pairs consisting of chloroacetonitrile and the alcohols methanol, ethanol, *n*- and *i*-propanol. Detailed calculations have been included for the  $(\text{ClCH}_2\text{CN})(\text{CH}_3\text{OH})\text{H}^+$  system for comparison to the  $(\text{CH}_3\text{CN})(\text{CH}_3\text{OH})\text{H}^+$  ion. The proton affinity (PA) of chloroacetonitrile is significantly lower than that of acetonitrile which will affect the relative energies of the possible simple-dissociation products and thus the degree to which it competes with the isomerization reaction. Not as obvious is the effect of chloro-substitution on the transition state leading to the  $\text{S}_{\text{N}}2$  isomerization products.

## 2. Experimental details

The experiments were performed on a modified triple sector VG ZAB-2HF mass spectrometer [5] incorporating a magnetic sector followed by two electrostatic sectors (BEE geometry). Protonated cluster ions were generated in the chemical ionization ion source of the instrument. The pressures in the ion source chamber, read with an ionization gauge located above the ion source diffusion pump, were typically between  $10^{-5}$  and  $10^{-4}$  Torr (the pressure in the ion source itself being approximately two orders of magnitude higher). Cluster ions were not observed when the pressure was below  $10^{-5}$  Torr, and there was no evidence of higher order clusters at any of the pressures used in these experiments. Metastable ion (MI)

and collision-induced dissociation (CID) mass spectra were recorded in the usual manner in both the second and third field-free regions (2FFR and 3FFR, respectively) of the instrument [6]. Helium collision gas was used in all CID experiments and was introduced into the collision cells to achieve 10% reduction in the ion flux (i.e., single collision conditions). All chemicals were commercially obtained and used without further purification.

## 3. Computational details

Standard ab initio molecular orbital calculations [7] were performed using the Gaussian 98 [8] suite of programs. Geometries were optimized, and harmonic vibrational frequencies were calculated at MP2/6-31+G(d) level of theory. Our previous work has shown that relative energies on these reaction surfaces are adequately described at this level of theory [1–3,9]. Transition states were confirmed by the intrinsic reaction coordinate method in Gaussian 98.

Unimolecular reaction rate constants were estimated using the standard RRKM expression [10]:

$$k(E) = \frac{\sigma N^\ddagger(E - E_0)}{h\rho(E)} \quad (1)$$

where  $N^\ddagger(E - E_0)$  is the transition state sum-of-states above the activation energy  $E_0$  and  $\rho(E)$  is the density of states of the reactant ion at an internal energy  $E$ . The sums and densities of states were obtained via the direct count algorithm of Beyer and Swinehart [11]. For isomerization reactions, the vibrational frequencies and relative energies of the reactant ions and the transition state structures were obtained from the ab initio calculations (vibrational frequencies were scaled by 0.943 prior to use [12]). The only unknowns are the vibrational frequencies for the effective transition states for the simple-bond cleavage reactions. Since

the RRKM calculations are being used for a qualitative understanding of the relative kinetics on the reaction surface, the transition state vibrational frequencies for simple cleavage reactions were estimated by employing the vibrational frequencies of the reactant ions and scaling the lowest five modes to achieve an entropy of activation,  $\Delta S^\ddagger(600\text{ K})$ , of  $+12\text{ J K}^{-1}\text{ mol}^{-1}$ . In addition, the vibration due to rotation about the hydrogen bond in the proton-bound pair was removed from both the reactant ion and approximated transition state and was treated as a hindered internal rotation [12].

#### 4. Results and discussion

The 2FFR MI mass spectrum of each ion,  $(\text{ClCH}_2\text{CN})(\text{CH}_3\text{OH})\text{H}^+$ ,  $(\text{ClCH}_2\text{CN})(\text{CH}_3\text{CH}_2\text{OH})\text{H}^+$ ,

$(\text{ClCH}_2\text{CN})(\text{CH}_3\text{CH}_2\text{CH}_2\text{OH})\text{H}^+$  and  $(\text{ClCH}_2\text{CN})((\text{CH}_3)_2\text{CHOH})\text{H}^+$  are shown in Fig. 1. In each case the isotopically pure  $^{35}\text{Cl}$  containing ions were selected.

##### 4.1. $(\text{ClCH}_2\text{CN})(\text{CH}_3\text{OH})\text{H}^+$

The chloroacetonitrile–methanol proton-bound ion (Fig. 1a)  $(\text{ClCH}_2\text{CN})(\text{CH}_3\text{OH})\text{H}^+$  (**1**),  $m/z$  108, exhibits two peaks,  $m/z$  90 (–18 amu) and  $m/z$  33 (–75 amu). The loss of 18 amu is attributed to the loss of water while the other peak is due to the loss of  $\text{ClCH}_2\text{CN}$  to form  $\text{CH}_3\text{OH}_2^+$ . The absence of a peak due to protonated chloroacetonitrile ( $m/z$  76) is consistent with the relative PA of methanol ( $754.3\text{ kJ mol}^{-1}$ ) and chloroacetonitrile ( $745.7\text{ kJ mol}^{-1}$ ) [13].

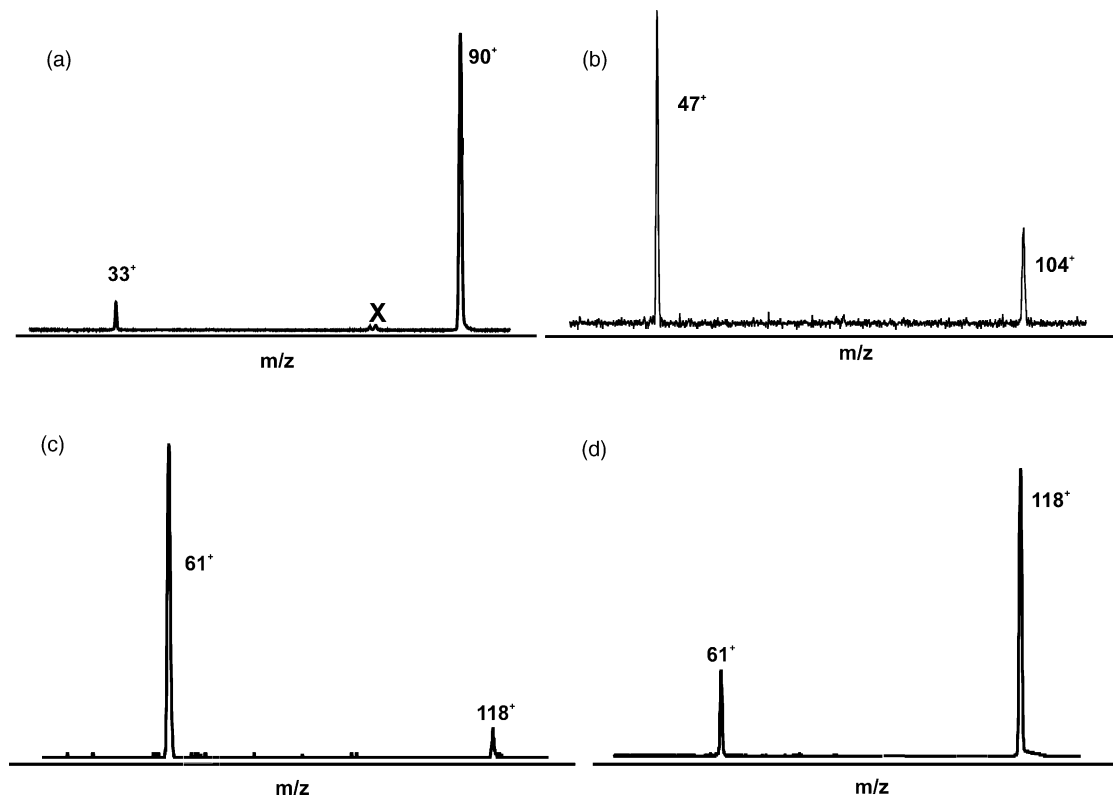


Fig. 1. MI mass spectra obtained in the second field free region of the VG ZAB-2HF of (a)  $(\text{ClCH}_2\text{CN})(\text{CH}_3\text{OH})\text{H}^+$ , (b)  $(\text{ClCH}_2\text{CN})(\text{CH}_3\text{CH}_2\text{OH})\text{H}^+$ , (c)  $(\text{ClCH}_2\text{CN})(\text{CH}_3\text{CH}_2\text{CH}_2\text{OH})\text{H}^+$  and (d)  $(\text{ClCH}_2\text{CN})((\text{CH}_3)_2\text{CHOH})\text{H}^+$ . Artifacts, denoted with an (X), are due to the  $^{13}\text{C}$  contribution of a peak in the mass spectrum one unit lower in mass.

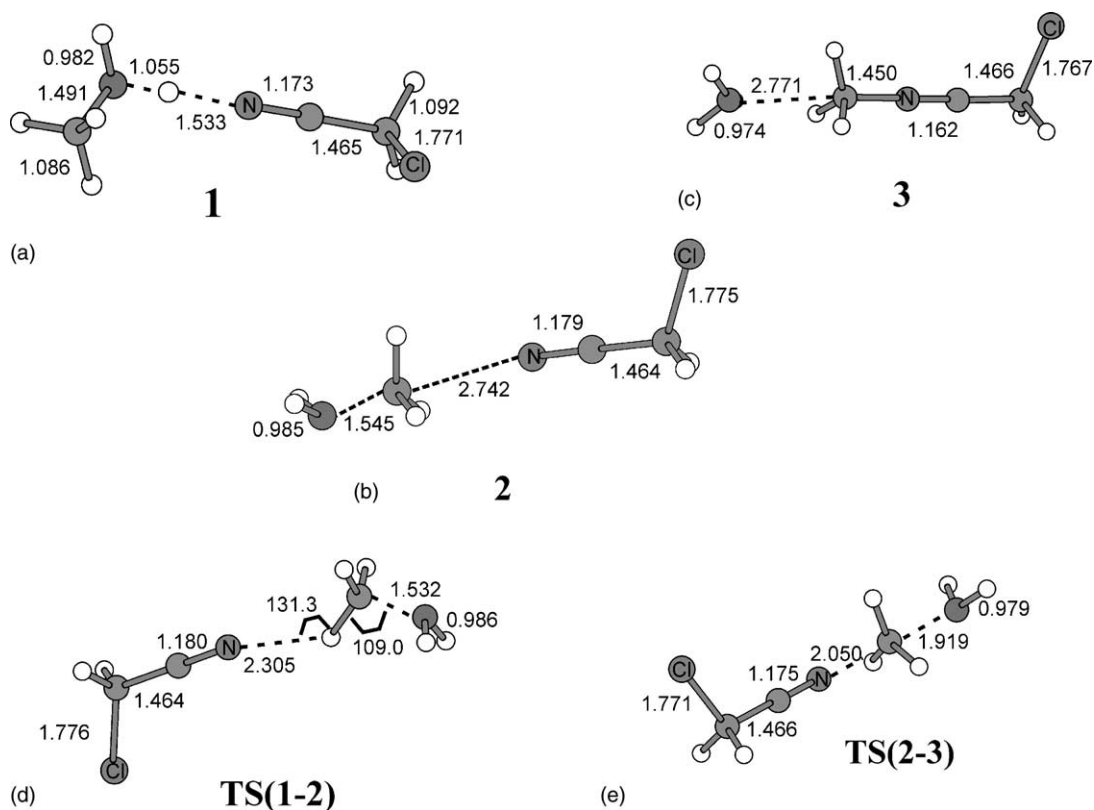


Fig. 2. Selected geometric parameters for the proton-bound dimer  $(\text{ClCH}_2\text{CN})(\text{CH}_3\text{OH})\text{H}^+$  (**1**), its isomers (**2**, **3**) and transition state structures **TS(1-2)** and **TS(2-3)**. All geometries were fully optimized at the MP2/6-31+G(d) level of theory. Bond lengths are in angstroms, bond angles in degrees.

Ab initio calculations were employed to map out the minimum energy reaction pathways for the  $(\text{ClCH}_2\text{CN})(\text{CH}_3\text{OH})\text{H}^+$  ion at the MP2/6-31+G(d) level of theory. Optimized structures for equilibrium and transition states are shown in Fig. 2 and relative energies are listed in Table 1. The reaction leading to water loss was assumed to proceed via an  $\text{S}_{\text{N}}2$ -type reaction similar to that observed for the acetonitrile-containing pairs (Scheme 1). The first step in the process involves a backside attack of  $\text{ClCH}_2\text{CN}$  on the carbon adjacent to the  $\text{OH}_2$  group in the protonated alcohol to form an intermediate complex **2** ( $\text{ClCH}_2\text{CN} \cdots \text{CH}_3 \cdots \text{OH}_2$ )<sup>+</sup> (via **TS(1-2)**, TSa). The second step involves the stretching of the C–O bond in the protonated alcohol and the shortening of the N–C bond (**TS(2-3)**, TSb), followed by the formation of the

Table 1

Calculated relative energies for the proton-bound pair  $(\text{ClCH}_2\text{CN})(\text{CH}_3\text{OH})\text{H}^+$ , its isomers, transition structures and fragmentation products

	Relative energy <sup>a</sup>
$(\text{ClCH}_2\text{CN})(\text{CH}_3\text{OH})\text{H}^+$ ( <b>1</b> )	0
$(\text{ClCH}_2\text{CN} \cdots \text{CH}_3 \cdots \text{OH}_2)^+$ ( <b>2</b> )	72
$(\text{ClCH}_2\text{CNCH}_3)(\text{H}_2\text{O})^+$ ( <b>3</b> )	–6
<b>TS(1-2)</b>	76
<b>TS(2-3)</b>	104
$\text{ClCH}_2\text{CNCH}_3^+$ ( <b>4</b> ) + $\text{H}_2\text{O}$	34
$\text{ClCH}_2\text{CNH}^+$ + $\text{CH}_3\text{OH}$	144
$\text{CH}_3\text{OH}_2^+$ + $\text{ClCH}_2\text{CN}$	123

<sup>a</sup> Values calculated at the MP2/6-31+G(d) level of theory incorporating scaled (by 0.943) MP2/6-31+G(d) zero-point vibrational energies (in  $\text{kJ mol}^{-1}$  at 0 K).

thermodynamically stable isomer **3** ( $\text{ClCH}_2\text{CNCH}_3$ ) ( $\text{H}_2\text{O}$ )<sup>+</sup>. Ion **3** dissociates to ion **4** ( $\text{ClCH}_2\text{CNCH}_3$ )<sup>+</sup> plus water. The transition state for the interconversion of the intermediate complex **2** to ion **3**, **TS(2-3)** lies  $104\text{ kJ mol}^{-1}$  above **1** and  $19\text{ kJ mol}^{-1}$  below the lowest energy simple-dissociation products ( $\text{CH}_3\text{OH}_2^+ + \text{ClCH}_2\text{CN}$ ).

The reaction pathways for the two proton-bound pairs ( $\text{ClCH}_2\text{CN})(\text{CH}_3\text{OH})\text{H}^+$  and  $(\text{CH}_3\text{CN})(\text{CH}_3\text{OH})\text{H}^+$  are compared in Fig. 3. Chloro-substitution on the acetonitrile has a small stabilizing effect on TSa and the intermediate ion in the  $\text{S}_{\text{N}}2$  mechanism but has no effect on the highest energy transition state leading to the water-loss products (TSb). The lowest energy simple-dissociation products become  $\text{CH}_3\text{OH}_2^+ + \text{ClCH}_2\text{CN}$ , which lie  $2\text{ kJ mol}^{-1}$  higher than  $\text{CH}_3\text{CNH}^+ + \text{CH}_3\text{OH}$  (relative to their respective proton-bound pairs). The calculations predict a difference in energy between the two channels ( $E_0(\text{dissociation}) - E_0(\text{isomerization})$ ) of  $19\text{ kJ mol}^{-1}$  in the chloro-substituted system compared to  $18\text{ kJ mol}^{-1}$  in the non-substituted system.

The  $1\text{ kJ mol}^{-1}$  difference between these values is insufficient to cause a dramatic shift in the relative abundance of the two reaction pathways (the MI mass spectra exhibit ratios for dissociation to isomerization of 1.0:0.5 for  $(\text{CH}_3\text{CN})(\text{CH}_3\text{OH})\text{H}^+$  [1] and 0.1:1.0 for  $(\text{ClCH}_2\text{CN})(\text{CH}_3\text{OH})\text{H}^+$ ). Chloro-substitution does reduce the relative energy of the initial transition state leading from the proton-bound pair to the intermediate ( $\text{ClCH}_2\text{CN}\cdots\text{CH}_3\cdots\text{OH}_2$ )<sup>+</sup> ion (TSa) by  $13\text{ kJ mol}^{-1}$ . While this step in the isomerization reaction is not rate limiting, it may influence the relative abundance of the two product channels.

To examine this possibility, the MP2/6-31+G(d) reaction surface was kinetically modeled with RRKM theory. Four elementary reactions were addressed: the reaction leading from **1** to  $\text{CH}_3\text{OH}_2^+ + \text{ClCH}_2\text{CN}$  ( $k_1$ ), the forward isomerization of **1** to **2** ( $k_2$ ), the reverse isomerization of **2** to **1** ( $k_3$ ) and the forward isomerization of **2** to **3** ( $k_4$ ). The individual rate constants are plotted as a function of the internal energy of **1** in Fig. 4a. Due to its small density of states the rate

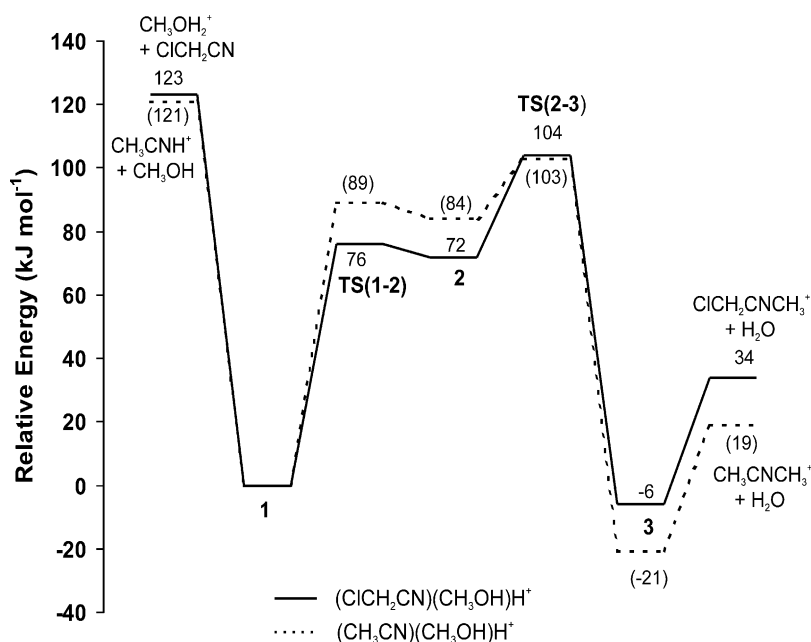


Fig. 3. Comparison the minimum energy reaction pathways of the proton-bound pairs  $(\text{ClCH}_2\text{CN})(\text{CH}_3\text{OH})\text{H}^+$  (solid line) and  $(\text{CH}_3\text{CN})(\text{CH}_3\text{OH})\text{H}^+$  (dashed line). All values are in  $\text{kJ mol}^{-1}$ .

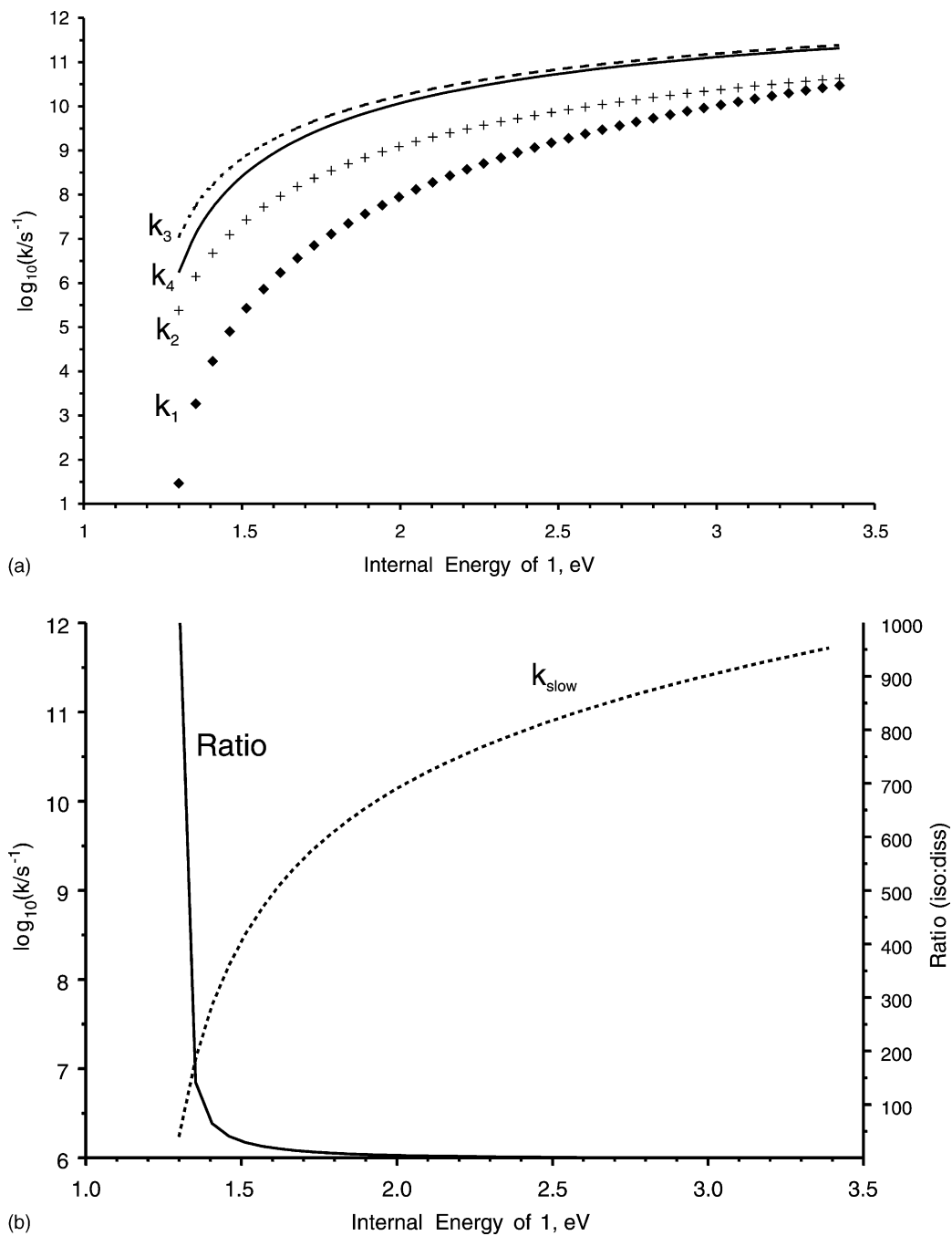


Fig. 4. (a) Plot of  $\log k$  vs.  $E$  curves for the four principle unimolecular reactions on the  $(\text{ClCH}_2\text{CN})(\text{CH}_3\text{OH})\text{H}^+$  surface  $k_1$  ( $\blacklozenge$ ),  $k_2$  ( $+$ ),  $k_3$  (---) and  $k_4$  (—) and (b) plot of  $\log k$  vs.  $E$  for  $k_{slow}$ .

constants for the reactions leading out from ion **2** ( $k_3$  and  $k_4$ ) are similar to each other and significantly greater than those for reactions from ion **1**. The two potential energy wells on the surface means that products will be formed with a biexponential rate consisting of fast and slow components. The fast component of the rate (having a rate constant  $k_{\text{fast}}$ ) will be due to the immediate dissociation of ion **1** to products via  $k_1$  prior to any isomerization reaction and will only be significant during the early stages of the reaction before the ions arrive in the 2FFR. Only the slow component of the rate (having a rate constant  $k_{\text{slow}}$ ) will be important in the 2FFR of the mass spectrometer. The value of  $k_{\text{slow}}$  is plotted in Fig. 4b and was calculated following the treatment developed by Baer et al. [14] for a two-well reaction surface. The rate of formation of the dehydration products ( $dP_{\text{iso}}/dt$ ) and the dissociation products ( $dP_{\text{diss}}/dt$ ) can be expressed as:

$$\frac{dP_{\text{iso}}}{dt} = k_4(e^{-\lambda_{\text{slow}}t} + e^{-\lambda_{\text{fast}}t}) \quad (2)$$

$$\frac{dP_{\text{diss}}}{dt} = k_1 \left( \frac{k_3 + k_4}{k_2} e^{-\lambda_{\text{slow}}t} + \frac{k_2}{k_3 + k_4} e^{-\lambda_{\text{fast}}t} \right) \quad (3)$$

where  $\lambda_{\text{fast}}$  and  $\lambda_{\text{slow}}$  are the eigenvalues of the  $2 \times 2$  matrix obtained for a 2-well surface (as derived by Baer et al. [14], case “C” with the rate constants renumbered accordingly). The equation for  $k_{\text{slow}}$  comes from the coefficients for the slow components in Eqs. (2) and (3) [14]:

$$k_{\text{slow}} = k_1 \left( \frac{k_3 + k_4}{k_2} \right) + k_4 \quad (4)$$

The ratio of water-loss products to simple-dissociation products, ratio (iso/diss), will be determined by the ratio of their respective rate constants:

$$\text{Ratio} \left( \frac{\text{iso}}{\text{diss}} \right) = \frac{k_4}{k_1(k_3 + k_4/k_2)} \quad (5)$$

This ratio is plotted in Fig. 4b. At internal energies below 1.5 eV, the isomerization channel dominates the chemistry of the proton-bound pair. The ratio drops to  $\sim 0.6$  at an internal energy of 3.5 eV. This is at least qualitatively consistent with the MI mass spectrum which reflects the dissociation of low-internal

energy ions on the microsecond timescale. Since there is considerable uncertainty about the internal energy distribution of metastable ions, a quantitative correlation cannot be made. In Eq. (5), as  $k_2$  decreases so does the ratio between isomerization and simple-bond cleavage. The relative energy of TSa is larger for the  $(\text{CH}_3\text{CN})(\text{CH}_3\text{OH})\text{H}^+$  ion than it is for the chloro-substituted ion (Fig. 3) and thus, a greater fraction of the  $(\text{ClCH}_2\text{CN})(\text{CH}_3\text{OH})\text{H}^+$  ions undergo dehydration.

Another possible explanation for the dominance of the isomerization channel in the chloro-substituted system is if  $\text{CH}_3\text{OH}_2^+$  reacts with  $\text{ClCH}_2\text{CN}$  in the ion source to form **2** directly. However, the population of **2** in the beam flux entering the 2FFR will be very small since, once formed, it rapidly isomerizes back to ion **1** (the ratio of  $k_3$  to  $k_2$  is greater than 40 at the low internal energies responsible for MI decomposition, Fig. 3).

#### 4.2. $(\text{ClCH}_2\text{CN})(\text{ROH})\text{H}^+$ ( $R = \text{CH}_3\text{CH}_2$ , $\text{CH}_3\text{CH}_2\text{CH}_2$ , $(\text{CH}_3)_2\text{CH}$ )

The 2FFR MI mass spectrum (Fig. 2b) of the chloroacetonitrile–ethanol proton-bound dimer ion  $(\text{ClCH}_2\text{CN})(\text{CH}_3\text{CH}_2\text{OH})\text{H}^+$  (**2**),  $m/z$  122, exhibits the same two basic reaction pathways as its methanol analogue, except that the simple dissociation to protonated ethanol dominates the spectrum. Methyl-substitution does not reduce the relative energy of TSb [3]. Chloro-substitution acts only to lower TSa and thus favors the isomerization reaction. Dominance of the simple-bond dissociation in the MI mass spectrum must therefore be due to the greater PA of ethanol ( $776.4 \text{ kJ mol}^{-1}$  versus  $754.3 \text{ kJ mol}^{-1}$  for methanol [13]) and hence lower dissociation-product energy.

The 2FFR MI mass spectra of the proton-bound pairs  $(\text{ClCH}_2\text{CN})(\text{CH}_3\text{CH}_2\text{CH}_2\text{OH})\text{H}^+$  and  $(\text{ClCH}_2\text{CN})((\text{CH}_3)_2\text{CHOH})\text{H}^+$  both exhibit peaks at  $m/z$  118 ( $-\text{H}_2\text{O}$ ) and  $m/z$  61 ( $-\text{ClCH}_2\text{CN}$ ), Figs. 2c and d. The relative intensities of the two competing channels in the *n*-propanol containing proton-bound pair are similar to those for the ethanol-containing

analogue. Ethyl-substitution of the central carbon in the  $(\text{CH}_3\text{CH}\cdots\text{R}\cdots\text{OH}_2)^+$  ion does not reduce the relative energy of TSb [3] and again the dominance of simple-bond dissociation products in Fig. 2c is due to the PA of the alcohol (PA of *n*-propanol is  $786.5 \text{ kJ mol}^{-1}$  versus  $754.3 \text{ kJ mol}^{-1}$  for methanol [13]). Dimethyl-substitution (*i*-propanol) does reduce the energy of TSb [3], and this effect is also apparent in the chloro-substituted system (Fig. 2d).

## 5. Conclusion

Proton-bound pairs of chloroacetonitrile and alcohols exhibit a competition on the microsecond timescale between simple-bond cleavage and isomerization leading to dehydration. The effect of chloro-substitution on acetonitrile does not significantly affect the height of the highest isomerization barrier governing the dehydration reaction. In the case of  $(\text{CH}_3\text{CN})(\text{CH}_3\text{OH})\text{H}^+$  the barrier lies approximately  $18 \text{ kJ mol}^{-1}$  below the lowest dissociation threshold  $(\text{CH}_3\text{CNH}^+ + \text{CH}_3\text{OH})$  while it is  $19 \text{ kJ mol}^{-1}$  lower for  $(\text{ClCH}_2\text{CN})(\text{CH}_3\text{OH})\text{H}^+$ . Chloro-substitution does reduce the proton affinity of acetonitrile resulting in the lowest energy simple-bond cleavage reaction products to be  $\text{ROH}_2^+ + \text{ClCH}_2\text{CN}$  in all cases. Kinetic modeling of the unimolecular reactions with RRKM theory showed that a key step in governing the ratio of the two types of reactions observed in the MI mass spectra is the initial rearrangement of the proton-bound pairs to the high energy intermediate structure  $(\text{CH}_3\text{CN}\cdots\text{R}\cdots\text{OH}_2)^+$ , even though it is not the rate-limiting step for the overall isomerization reaction leading to dehydration.

## Acknowledgements

PMM thanks the Natural Sciences and Engineering Research Council of Canada for continued funding.

## References

- [1] P.M. Mayer, J. Phys. Chem. A 103 (1999) 3687.
- [2] R.A. Ochran, A. Annamalai, P.M. Mayer, J. Phys. Chem. A 104 (2000) 8505.
- [3] R.A. Ochran, P.M. Mayer, Eur. Mass Spectrom. 7 (2001) 267.
- [4] T.D. Fridgen, J.D. Keller, T.B. McMahon, J. Phys. Chem. A (2001) 3816.
- [5] J.L. Holmes, P.M. Mayer, J. Phys. Chem. 99 (1995) 1366.
- [6] K.L. Busch, G.L. Glish, S.A. McLuckey (Eds.), Mass Spectrometry/Mass Spectrometry, VCH Publishers, New York, 1988.
- [7] W.J. Hehre, L. Radom, P.V.R. Schleyer, J.A. Pople (Eds.), Ab Initio Molecular Orbital Theory, Wiley, New York, 1986.
- [8] M.J. Frisch, G.W. Trucks, H.B. Schlegel, G.E. Scuseria, M.A. Robb, J.R. Cheeseman, V.G. Zakrzewski, J.A. Montgomery, R.E. Stratmann, J.C. Burant, S. Dapprich, J.M. Millam, A.D. Daniels, K.N. Kudin, M.C. Strain, O. Farkas, J. Tomasi, V. Barone, M. Cossi, R. Cammi, B. Mennucci, C. Pomelli, C. Adamo, S. Clifford, J. Ochterski, G.A. Petersson, P.Y. Ayala, Q. Cui, K. Morokuma, D.K. Malick, A.D. Rabuck, K. Raghavachari, J.B. Foresman, J. Cioslowski, J.V. Ortiz, B.B. Stefanov, G. Liu, A. Liashenko, P. Piskorz, I. Komaromi, R. Gomperts, R.L. Martin, D.J. Fox, T. Keith, M.A. Al-Laham, C.Y. Peng, A. Nanayakkara, C. Gonzalez, M. Challacombe, P. M.W. Gill, B. Johnson, W. Chen, M.W. Wong, J.L. Andres, C. Gonzalez, M. Head-Gordon, E.S. Replogle, J.A. Pople, GAUSSIAN 98 Rev. A.7, Gaussian Inc., Pittsburgh, PA, 1998.
- [9] P.M. Mayer, Chem. Phys. Lett. 314 (1999) 311.
- [10] T. Baer, W.L. Hase, Unimolecular Reaction Dynamics, Theory and Experiments, Oxford University Press, New York, 1996.
- [11] T. Beyer, D.R. Swinehart, ACM Commun. 16 (73), 379.
- [12] A.P. Scott, L. Radom, J. Phys. Chem. 100 (1996) 16502.
- [13] E.P. Hunter, S.G. Lias, in: P.J. Linstrom, W.G. Mallard (Eds.), Proton affinity evaluation NIST chemistry webbook, NIST standard reference database number 69, July 2001, National Institute of Standards and Technology, Gaithersburg MD, 20899 (<http://webbook.nist.gov>).
- [14] T. Baer, W.A. Brand, T.L. Bunn, J.J. Butler, Faraday Discuss. Chem. Soc. 75 (1983) 45.